Appl Microbiol Biotechnol (2010) 87:595–607
DOI 10.1007/s00253-010-2472-z

BIOTECHNOLOGICALLY RELEVANT ENZYMES AND PROTEINS

Characterization of the versatile monooxygenase CYP109B1 from *Bacillus subtilis*

Marco Girhard · Tobias Klaus · Yogan Khatri · Rita Bernhardt · Vlada B. Urlacher

Received: 26 October 2009 / Revised: 25 January 2010 / Accepted: 25 January 2010 / Published online: 26 February 2010

Abstract The oxidizing activity of CYP109B1 from *Bacillus subtilis* was reconstituted in vitro with various artificial redox proteins including putidaredoxin reductase and putidaredoxin from *Pseudomonas putida*, truncated bovine adrenodoxin reductase and adrenodoxin, flavodoxin reductase and flavodoxin from *Escherichia coli*, and two flavodoxins from *B. subtilis* (YkuN and YkuP). Binding and oxidation of a broad range of chemically different substrates (fatty acids, *n*-alkanes, primary *n*-alcohols, terpenoids like (+)-valencene, α- and β-ionone, and the steroid testosterone) were investigated. CYP109B1was found to oxidize saturated fatty acids (conversion up to 99%) and their methyl and ethyl esters (conversion up to 80%) at subterminal positions with a preference for the carbon atoms C11 and C12 counted from the carboxyl group. For the hydroxylation of primary *n*-alcohols, the ω_{-2} position was preferred. *n*-Alkanes were not accepted as substrates by CYP109B1. Regioselective hydroxylation of terpenoids α-ionone (~70% conversion) and β-ionone (~ 91% conversion) yielded the allylic alcohols 3-hydroxy-α-ionone and 4-hydroxy-β-ionone, respectively. Furthermore, indole was demonstrated to inhibit fatty acid oxidation.

Keywords *Bacillus subtilis* · P450 monooxygenase · Fatty acid · Terpene · Ionone · Activity reconstitution

Introduction

Cytochromes P450 (P450s or CYPs) belong to an ever-growing superfamily of heme *b* containing monooxygenases found in all domains of life (Nelson 2006). They play a central role in drug metabolism and are involved in the biosynthesis of important natural compounds. Currently, there are more than 11,800 P450 sequences available in several online databases, for example in CYPED (http://www.cyped.uni-stuttgart.de, Institute of Technical Biochemistry, Universitaet Stuttgart; Fischer et al. 2007; Sirim et al. 2009) or the P450 homepage maintained by Dr. Nelson (http://drnelson.utmem.edu/CytochromeP450.html, Molecular Sciences, University of Tennessee; Nelson 2006). P450s catalyze the introduction of one atom of molecular oxygen in organic molecules, while the second one is reduced to water. The basic P450 catalyzed reactions include hydroxylation of sp3-C atoms, heteroatom oxygenation, epoxidation of double bonds, and dealkylation (heteroatom release) (Cryle et al. 2003). Two electrons in form of hydride ions required for the P450 catalysis are in most cases delivered from the pyridine cofactors NAD(P)H via flavoprotein and/or iron–sulfur redox partners. Traditionally, P450s are classified depending on the topology of the protein components involved in the electron transfer from NAD(P)H to the heme iron. The classical system distinguished two major classes of P450s: Mitochondrial and most bacterial P450s (class I) comprising an iron–sulfur ferredoxin and a flavin adenine dinucleotide (FAD)-containing ferredoxin reductase; and microsomal P450s (class II) with a membrane-bound, FAD-, and flavin

Electronic supplementary material The online version of this article (doi:10.1007/s00253-010-2472-z) contains supplementary material, which is available to authorized users.

M. Girhard · T. Klaus · V. B. Urlacher (✉)
Institute of Technical Biochemistry, Universitaet Stuttgart,
Allmandring 31,
70569 Stuttgart, Germany
e-mail: Vlada.Urlacher@itb.uni-stuttgart.de

Y. Khatri · R. Bernhardt
Institute of Biochemistry, Saarland University,
66041 Saarbrücken, Germany

mononucleotide (FMN)-containing diflavin reductase. However, the recent discovery of a vast variety of novel P450s has introduced many new redox partner systems. Consequently, a more detailed classifying system is required, for example, a classification comprising ten different P450 classes that was recently suggested by Bernhardt and coworkers (Hannemann et al. 2007).

The monooxygenase described in this paper—CYP109B1—was identified in 1997, when the complete genome of the *Bacillus subtilis* strain 168 was sequenced (Kunst et al. 1997). The closest relative monooxygenase is CYP109A1 from the *B. subtilis* strain W23, which demonstrates 43% identity to CYP109B1 (Lawson et al. 2004a). CYP109B1 has a potential for the production of secondary metabolites since its ability to hydroxylate compactin to pravastatin (Endo et al. 2000) and to oxidize testosterone at position C15β (hydroxy-group) and C17 (keto-group) (Agematu et al. 2006; Arisawa and Agematu 2007) has been reported. Furthermore, FT-ICR/MS analysis applied for all P450s originating from *B. subtilis* demonstrated the ability of CYP109B1 to oxidize androsta-1,4-diene-3, 17-dione, norethindrone, methyltestosterone, testosterone enanthate, betamethasone dipropionate, and medroxyprogesterone acetate. However, the oxidation products for the latter substrates have not been identified (Furuya et al. 2008). Recently, we have demonstrated oxidation of (+)-valencene to nootkatol and (+)-nootkatone catalyzed by CYP109B1 (Girhard et al. 2009). (+)-Nootkatone is a high added value commercial flavoring (Fraatz et al. 2009), which reveals also a potential use of CYP109B1 for the production of fine chemicals in flavor and fragrance industries.

Although there is obviously a significant potential for the application of CYP109B1 in biotechnological processes, a systematic analysis concerning substrate binding and conversion has not been carried out so far. Furthermore, there is also a lack of knowledge regarding the electron transfer partners for this P450. Since the natural electron transfer proteins for CYP109B1 have not been identified yet, "artificial" redox systems with putidaredoxin reductase (PdR) and putidaredoxin (Pdx) from *Pseudomonas putida* were employed in all published studies mentioned above (Agematu et al. 2006; Arisawa and Agematu 2007; Endo et al. 2000; Furuya et al. 2008; Girhard et al. 2009).

Herein, we report the identification and application of various electron transfer proteins of CYP109B1 for the significant improvement of substrate conversion in comparison to the PdR–Pdx system. Furthermore, binding and oxidation of various substrates by CYP109B1 was investigated (Fig. 1), and oxidized products were identified. The screening of substrates included saturated fatty acids **1–8**, fatty acid methyl **9–11** and ethyl esters **12–13**, unsaturated fatty acids **14–16**, primary *n*-alcohols **17–19**, and *n*-alkanes **20–22**, the sesquiterpene (+)-valencene **23**, the terpenoids α-ionone **25**, and β-ionone **26**, the heteroaromatic compounds coumarine **27**, naphthalene **28**, and indole **29**, as well as the steroid testosterone **30**.

Materials and methods

Bacterial strains, expression vectors, enzymes, and chemicals

Escherichia coli DH5α (F^- *supE44* Δ*lacU169* (ϕ*80lacZ*Δ*M15) hsdR17 recA1 endA1 gyrA96 thi-1 relA1*; Invitrogen, Karlsruhe, Germany) was used as host for cloning purposes. *E. coli* BL21(DE3) (F^- *ompT* $hsdS_B(r_B^- m_B^-)$ *gal dcm* (DE3); Novagen, Darmstadt, Germany) was used for recombinant gene expression. The expression vectors pET11a, pET16b, and pET28a(+) were bought from Novagen. Restriction endonucleases, T4 DNA ligase, *Pfu* DNA polymerase, and isopropyl-β-D-thiogalactopyranoside (IPTG) were obtained from Fermentas (St. Leon-Rot, Germany). NADH and NADPH were from Codexis (Jülich, Germany). Glucose-6-phosphate dehydrogenase from *Saccharomyces cerevisiae* was from Roche Diagnostics (Mannheim, Germany). Glucose-6-phosphate dehydrogenase from *Leuconostoc mesenteroides* and all other chemicals, solvents, and buffer components were purchased from Sigma-Aldrich (Schnelldorf, Germany).

Molecular biological techniques, protein expression, and purification

General molecular biology manipulations and microbiological experiments were carried out by standard methods (Sambrook and Russell 2001).

Expression and purification of CYP109B1, PdR, and Pdx

Constructions of the following plasmids, protein expressions, and purifications were carried out as described previously (Girhard et al. 2009): pET28a-CYP109B1 for expression of the CYP109B1-encoding *yjiB* gene (GeneBank CAB13078) from *B. subtilis* strain 168 DSM 402 (GeneBank NC_000964); pET28a-camA for expression of the PdR-encoding *camA* gene (EMBL-Bank BAA00413) from *P. putida* ATCC 17453; and pET28a-camB for expression of the Pdx-encoding *camB* gene (EMBL-Bank BAA00414) from *P. putida* ATCC 17453.

Expression and purification of the reductase domain of CYP102A1

The plasmid pET28a-CYPRed for expression of the reductase domain (BMR) of CYP102A1 from *Bacillus*

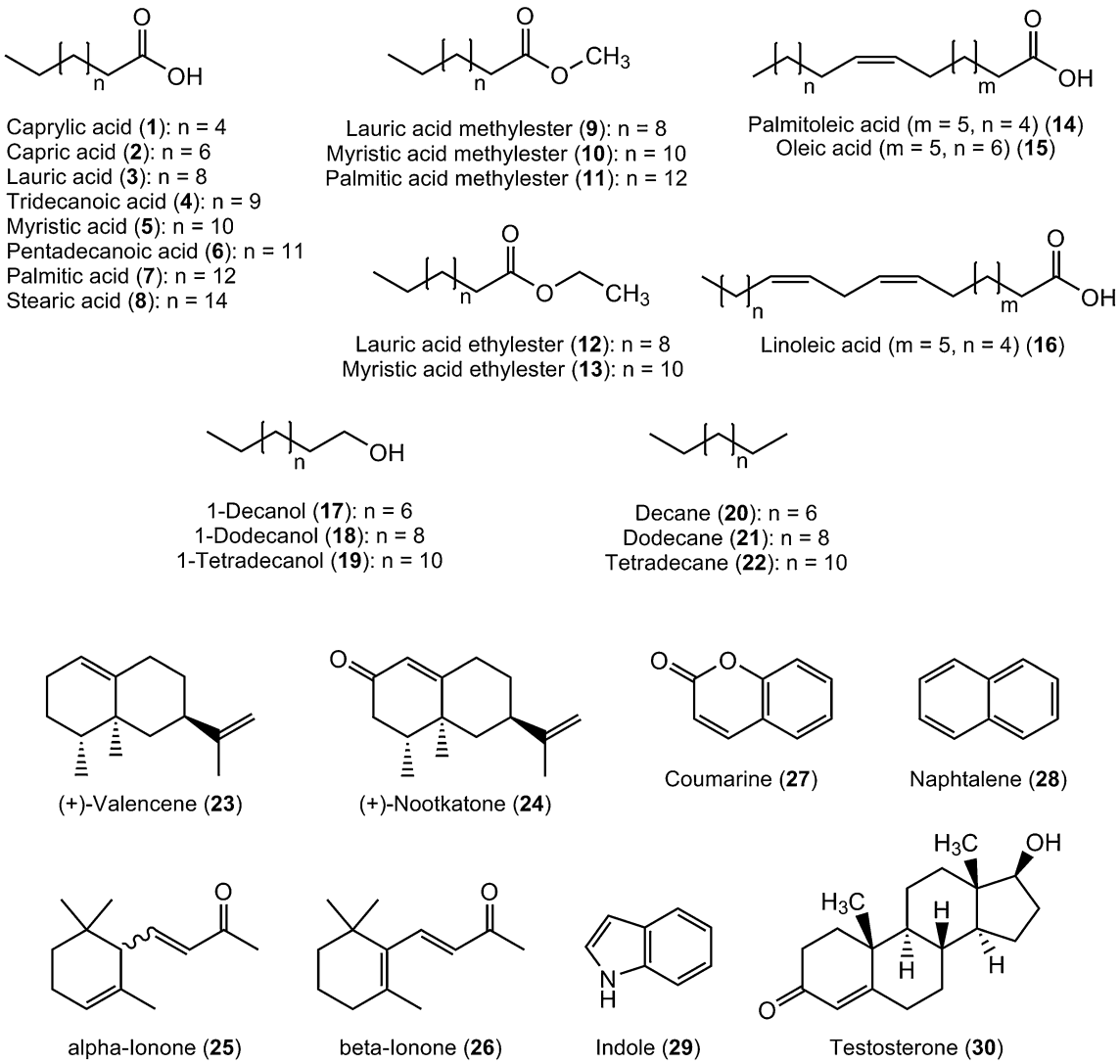

Fig. 1 Substances investigated with CYP109B1

megaterium ($P450_{BM3}$) was constructed by insertion of the part of the CYP102A1 gene (GeneBank J04832.1) coding for the diflavin reductase into pET28a(+). Assembly of the construct, protein expression, and purification has been described previously (Girhard et al. 2007; Maurer et al. 2003).

Expression and purification of flavodoxin reductase and flavodoxin from E. coli

Flavodoxin (Fdx) from *E. coli* JM109 was expressed from pET11a containing the corresponding gene. Expression and purification was carried out as described elsewhere (Jenkins and Waterman 1998).

Flavodoxin reductase (FdR) from *E. coli* JM109 was inserted into pET16b as follows: The plasmid pET11a-*fpr* as described (Jenkins and Waterman 1998) was utilized as DNA template for a polymerase chain reaction (PCR), together with the forward 5′-GTATcc**atg**gGCCATCATC ATCATCATCATGCTGATTGGGTA-3′, which introduced an *Nco*I site at the start codon and six additional histidines (underlined), and the reverse primer 5′-GATAggatcc**TTA**C CAGTAATGCTCCGCTGTCAT-3′, which introduced *Bam*HI at the 3′ end. The PCR was performed with *Pfu* DNA polymerase under the following conditions: 95°C for 3 min; 30 cycles of 95°C for 1 min, 57±2°C for 45 s, 72°C for 2 min; and finally 72°C for 3 min. The PCR product was purified, digested with endonucleases *Nco*I and *Bam*HI, and inserted into previously linearized pET16b. The resulting DNA construct, pET16b-FdR, was sequenced by automated DNA sequencing (GATC-Biotech, Konstanz, Germany) and encoded for N-terminally His6-tagged FdR. For expression of recombinant FdR, *E. coli* BL21(DE3) cells were transformed with pET16b-FdR, spread onto Luria broth (LB) agar plates containing 100 μg ml^{-1} ampicillin, and grown overnight at 37°C. 400 ml of LB-medium

supplemented with 100 μg ml^{-1} ampicillin were inoculated with 2 ml of an overnight culture—grown from a single colony—and incubated at 37°C, 180 rpm to an optical density at 600 nm of approximately 0.6. IPTG (100 μM) were added, and the culture was grown for another 19 h at 25°C, 150 rpm. Cells were harvested by centrifugation at 10,800×g for 20 min at 4°C. The supernatant was discarded, and cell pellet was resuspended in 10-ml purification buffer (50 mM Tris–HCl, pH 7.5, 500 mM NaCl, 5% glycerol, 100 μM phenylmethanesulfonyl fluoride (PMSF)). Cells were disrupted by sonication on ice (6×30-s bursts, interspaced by 1.5 min), cell debris was removed by centrifugation, and the soluble protein fraction was recovered and filtered through a 0.45-μm filter. FdR was purified from the soluble protein fraction by immobilized metal affinity chromatography (IMAC) using a Talon® resin (7-ml bed volume). The protein lysate was applied to the column, which was pre-equilibrated with 6-column volumes of purification buffer. Nonspecifically bound proteins were washed off the column with 4-column volumes of purification buffer containing 20 mM imidazol, before the bound protein was eluted with 2 column volumes of purification buffer with 100 mM imidazol. Fractions containing FdR were pooled, dialyzed twice against 1.5 l of 50 mM Tris–HCl, pH 7.5, 5% glycerol, 100 μM PMSF, and 100 μM dithiothreitol at 4°C. Aliquots of the purified protein were prepared and frozen at −20°C until use.

Expression and purification of AdR and Adx

The mammalian truncated $Adx_{4–108}$ (Uhlmann et al. 1994) and AdR were expressed and purified as described before (Hannemann et al. 2002; Sagara et al. 1993).

Expression and purification of YkuN and YkuP

Oligonucleotide primers for the amplification of the *ykuN* and *ykuP* genes from *B. subtilis* strain 168 were designed through analysis of the respective gene sequences using the "SubtiList" genome database (http://genolist.pasteur.fr/SubtiList/). pET16b-YkuN(+)—a vector for the expression of recombinant YkuN—was constructed as follows: The *ykuN*-gene was amplified from genomic DNA of the *B. subtilis* strain 168 by PCR using a forward 5′-GAActcgag ATGGCTAAAGCCTTGATTAC-3′ and reverse primer 5′-GCCggatcc**TTA**TGAAACATGGATTTTTTCC-3′. PCR conditions were as follows: 95°C for 5 min; 25 cycles of 95°C for 1 min, 57°C for 30 s, 72°C for 2 min; 72°C for 3 min. The PCR product was purified, digested with endonucleases *Xho*I and *Bam*HI, and inserted into previously linearized pET16b. The resulting DNA construct encodes for N-terminally His10-tagged YkuN under control of the IPTG-inducible T7 phage promoter.

The basic steps for construction of pET16b-YkuP(+)—a vector for the expression of recombinant YkuP—were identical with those of pET16b-YkuN(+), except that the forward 5′-GAActcgagGCGAAGATTTTGCTCGTTTATG-3′ and reverse primer 5′-CCggatcc**CTA**CCTCATTACTG TATCAAAGG-3′ were used for PCR.

Both plasmid constructs were verified by automated DNA sequencing. The DNA sequence alignments of the obtained sequences for *ykuN* were in agreement with those reported in the "SubtiList" genome database. Furthermore, the sequencing of *ykuP* confirmed the absence of one adenine nucleotide at position 436—as discovered by Lawson et al. (2004b)—leading to a change in reading frame to obtain a corrected *ykuP* gene. This gene codes for a protein of 151 amino acids with a molecular mass of 16.9 kDa, instead of 178 amino acids and 20.2 kDa as predicted from genome sequencing (Kunst et al. 1997).

Expression of recombinant YkuN and YkuP, IMAC purification, and dialysis were carried out as described for FdR but with 50 mM Tris–HCl, pH 7.5, 5% glycerol, 100 μM PMSF as dialysis buffer. Aliquots of the purified proteins were stored at −20°C until use.

Determination of protein concentration

The expression level of CYP109B1 was estimated using the CO-difference spectral assay as described previously with $\varepsilon_{450–490}$=91 $mM^{-1}cm^{-1}$ (Omura and Sato 1964a; Omura and Sato 1964b; the ferrous–CO spectrum of CYP109B1 is shown in Fig. S1 of the Electronic Supplementary Material). Using this value, the extinction coefficient for the ferric resting state of CYP109B1 was calculated to be ε_{418}=128 $mM^{-1}cm^{-1}$ and was applied for the determination of spin-state shifts upon substrate binding.

The concentration of PdR was determined as the average of the concentration calculated from each of the three wavelengths 378, 454, and 480 nm using extinction coefficients (ε) 9.7, 10.0, and 8.5 $mM^{-1}cm^{-1}$ (Purdy et al. 2004). The concentration of Pdx was determined as the average concentration calculated with ε_{415}=11.1 $mM^{-1}cm^{-1}$ and ε_{455}=10.4 $mM^{-1}cm^{-1}$ (Purdy et al. 2004). The concentration of BMR was calculated as average concentration determined from ε_{452}=10.0 $mM^{-1}cm^{-1}$ and ε_{466}= 10.0 $mM^{-1}cm^{-1}$ (Sevrioukova et al. 1996).

Fdx concentration was estimated at 465 nm with ε= 8420 $M^{-1}cm^{-1}$ (Fujii and Huennekens 1974). For FdR, the concentration was determined at 456 nm with ε=7.1 $mM^{-1}cm^{-1}$ (McIver et al. 1998). Adx and AdR concentrations were determined using the molar extinction coefficients ε_{415}= 9.8 $mM^{-1}cm^{-1}$ (Huang and Kimura 1973) and ε_{450}= 10.9 $mM^{-1}cm^{-1}$ (Chu and Kimura 1973), respectively. YkuN and YkuP concentrations were determined at 461 nm with ε= 10 $mM^{-1}cm^{-1}$ (Lawson et al. 2004b; Wang et al. 2007).

Spin-state shift and substrate dissociation constant determinations

Spin-state shifts upon substrate binding were assayed at 25°C under aerobic conditions using an UV–VIS scanning photometer (UV-2101PC, Shimadzu, Japan) equipped with two tandem quartz cuvettes (Hellma, Müllheim, Germany) simultaneously. One chamber of each cuvette contained 10 μM CYP109B1 in buffer (50 mM Tris–HCl, pH 7.5), whereas the second chamber contained buffer alone. The initial volume was 800 μl. Substrates were dissolved in DMSO, except for stearic acid **8** and testosterone **30**, which were dissolved in ethanol. Substrate titrations where done by adding small (<5 μl) aliquots of an appropriate stock of a substrate or ligand into the P450 containing chamber of the sample cuvette. An equal amount of solvent was added into the buffer containing chamber of the reference cuvette, and spectral changes between 350 and 500 nm were recorded. When saturation of CYP109B1 with a substrate was achieved, substrate dissociation constants (K_D) were calculated by fitting the data to the hyperbolic equation (Eq. 1):

$$\Delta A = \frac{\Delta A \max \times [S]}{KD + [S]} \quad (1)$$

ΔA is the peak-to-trough difference in absorbance, ΔA_{max} is the maximum difference in absorbance, and [S] is the concentration of the substrate.

Reconstitution of CYP109B1 activity in vitro

Various enzyme systems were applied to reconstitute the in vitro activity of CYP109B1. The basic setup for determination of the NAD(P)H consumption rate and coupling within the reconstituted systems was as follows: 1 μM reductase, 10 μM flavo- or ferredoxin, 1 μM CYP109B1, 4 mM glucose-6-phosphate,1 mM $MgCl_2$, 200 μM substrate (from a 10 mM stock solution in DMSO or ethanol) were mixed in 50 mM Tris–HCl, pH 7.5 to a final volume of 250 μl in a 96-microwell plate. After incubation at 30°C for 2 min, 200 μM NAD(P)H were added, and the absorption was followed at 340 nm. The NAD(P)H consumption rate was calculated using ε=6.22 $mM^{-1} cm^{-1}$. After all NAD(P)H was consumed, the internal standard (final concentration 50 μM) was added, and samples were prepared for quantitative gas–liquid chromatography/mass spectrometry (GC/MS) analysis to determine the coupling efficiency.

For product identification and determination of conversion, the basic setup was as follows: 1 μM reductase, 10 μM flavo- or ferredoxin, 1 μM CYP109B1, 5 U of glucose-6-phosphate dehydrogenase from *S. cerevisiae* (for regeneration of NADPH) or from *L. mesenteroides* (for regeneration of NADH), 4 mM glucose-6-phosphate, and 1 mM $MgCl_2$ were mixed in a 1.5-ml reaction tube and incubated at 30°C for 2 min. 50 mM Tris–HCl, pH 7.5 and 200 μM substrate were added to a final volume of 500 μl. The reaction was started by addition of 200 μM NADH or NADPH, and samples were incubated at 30°C for 15 min to 2 h. After incubation, the internal standard (final concentration 50 μM) was added, and samples were prepared for product analysis.

For saturated, unsaturated fatty acids, and primary *n*-alcohols, the reaction was stopped by addition of 20 μl 37% HCl. Internal standards were used as follows: **4** in the case of **5**, **6**, **7**, **8**, **10**, **11**, and **13**; **2** in the case of **3**, **4**, **9**, and **12**; **1** in the case of **2**; **17** in the case of **18** and **19**; **19** in the case of **17**. The reaction mixtures were extracted with 1 ml diethyl ether, dried over anhydrous $MgSO_4$, and the organic phases were evaporated. The residues were dissolved in 40 μl *N*,*O*-bis(trimethylsilyl)trifluoroacetamide containing 1% trimethylchlorosilane for derivatization, transferred into GC vials, and incubated at 80°C for 30 min prior to analysis.

Samples containing compounds **20–30** were extracted with 400 μl ethyl acetate. (−)-Carvone was used as internal standard for **23**, **25** served as internal standard for **26**, and vice versa. The organic phases were recovered and transferred into GC vials for product analysis.

Product analysis

The analysis of conversion products was carried out by GC/MS on a GC/MS-QP2010 (Shimadzu, Tokyo, Japan), equipped with a FS-Supreme-5 column (30 m×0.25 mm×0.25 μm, Chromatographie Service GmbH, Langerwehe, Germany). The injector and detector temperatures were set at 250°C and 285°C, respectively, with helium as carrier gas. Sample (1 μl) was injected for analysis. Conversion products were identified by their characteristic mass fragmentation patterns.

For quantification of the substrates, the detector response was calibrated with internal standards. Therefore, mixtures of 50 mM Tris–HCl buffer, pH 7.5, containing the respective substrate for calibration in final concentrations of 10 to 200 μM together with the respective internal standard in a final concentration of 50 μM were treated as described for normal conversion reactions and analyzed by GC/MS. The ratio of the area of the substrate to that of the internal standard was plotted against the substrate concentration to give a straight-line calibration plot.

For fatty acids and primary *n*-alcohols, a split of 30 was used. For **1**, **2**, **3**, **4**, **9**, **12**, **18**, and **19**, the column temperature was maintained at 130°C for 2 min, ramped to 250°C at a rate of 10°C min^{-1}, and held at 250°C for 3 min. For **5**, **6**, **7**, **8**, **10**, **11**, **13**, and **14–16**, the column

temperature was maintained at 180°C for 2 min, increased to 300°C at a rate of 8°C min^{-1}, and held at 300°C for 5 min. For **17** and **20–22**, a starting temperature of 110°C was maintained for 2 min, raised to 220°C at a rate of 10°C min^{-1}, and kept at this temperature for 2 min.

23 was injected at a split of 4. The column temperature was maintained at 120°C for 4 min, ramped to 250°C at a rate of 10°C min^{-1}, and held at 250°C for 5 min. For **25** and **26**, the split was 5. The column temperature was controlled at 130°C for 2 min, then raised to 230°C at a rate of 20°C min^{-1} and kept for 2 min.

In the case of **27** and **28**, injections were done with a split of 4. The column temperature was maintained at 120°C for 4 min, increased to 250°C at a rate of 10°C min^{-1}, and held at 250°C for 5 min. **29** was injected at a split of 10. The column temperature was maintained at 80°C for 4 min, ramped to 250°C at a rate of 8°C min^{-1}, and held for 4 min.

Results

Expression, purification, and spectral characterization of CYP109B1

The recombinant expression of CYP109B1 was performed in *E. coli* BL21(DE3) using the expression vector pET28a (+). The monooxygenase was purified by immobilized metal affinity chromatography (Fig. S2 of the Electronic Supplementary Material). The expression yield of CYP109B1 determined from CO-difference spectra was 3,570 nmol l^{-1} (160 mg l^{-1}). CYP109B1 showed a characteristic absorption at 452 nm for the $Fe^{II}(CO)$ complex with no evidence of the inactive P420 form. Photometric characterization of the purified CYP109B1 revealed spectra typical for a P450 monooxygenase (Fig. S1 of the Electronic Supplementary Material).

Determination of substrate binding constants

Substrate binding by P450s is often characterized by a spin-state shift of the Soret band from approximately 418 nm (representing the low-spin substrate free form) to around 390 nm for the high-spin form when a substrate is bound in close proximity to the heme, which results in a classical type I spectrum (Schenkman et al. 1981). Therefore, this method was used to identify potential CYP109B1 substrates.

A variety of saturated and unsaturated fatty acids showed type I binding to CYP109B1 (Fig. 2). The substrate dissociation constants (K_D) were determined as described in the Material and Methods section. The lowest K_D for saturated fatty acids of 230 μM was calculated for palmitic acid **7**. Saturated fatty acids with shorter or longer chain lengths showed weaker binding, and subsequently higher K_D

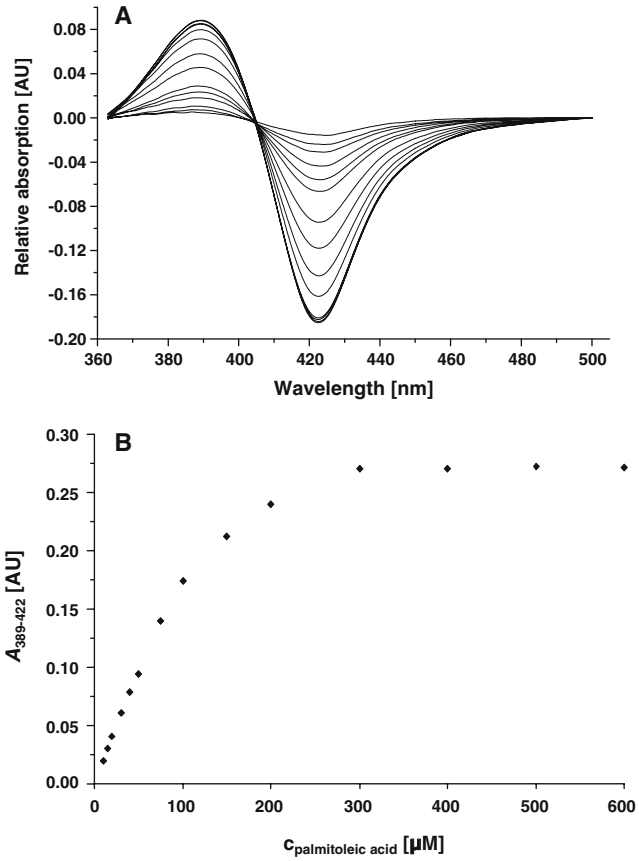

Fig. 2 **a** Type I substrate binding of palmitoleic acid **14** to CYP109B1. Peak and trough were observed at 389 and 422 nm for this substrate, respectively. **b** Peak-to-trough absorbance differences plotted against the respective palmitoleic acid concentration assayed

values were calculated for those substrates (Table 1). The unsaturated fatty acids **14–16** tested showed in general better binding to CYP109B1 than saturated fatty acids, which is reflected in lower K_D values calculated for those substrates.

Type I binding was also observed for α-ionone **25** and β-ionone **26**, and K_D values of 205 or 180 μM were calculated, respectively, indicating that CYP109B1 shows a slight preference for the binding of β-ionone **26** over α-ionone **25**. Tight binding with lowest K_D value of 24.5 μM was calculated for indole **29**, whereas no spin-state shifts were induced for coumarine **27** and naphthalene **28**.

As seen in Table 1, none of the substrates tested induced a full spin-state shift from low-spin in the absence of substrate to high-spin. The strongest shift of ~55% was observed for myristic acid. Other substrates resulted in lower high-spin heme content. In most cases, the percentage of the enzyme in high-spin state correlates to the calculated binding constants (Table 1).

Interestingly, no spin-state shifts were observed when testosterone **30** or (+)-valencene **23** were used for the binding experiment, although these substances are con-

Table 1 Type I spin-state shift values and binding constants for CYP109B1

Type of substrate	Chain length or name (no.)	K_D (μM)	Spin-state shift (%)[a]
Saturated fatty acids	8 (1)	(+)	(+)
	10 (2)	(+)	(+)
	12 (3)	3670±440	25
	13 (4)	1970±250	35
	14 (5)	1190±100	55
	15 (6)	720±55	15
	16 (7)	228±27	10
	18 (8)	983±67	7
Unsaturated fatty acids	16 (14)	115±13	8
	18 (15)	50±3	20
	18 (16)	12±1	25
Terpenoids	Valencene (23)	–	–
	Nootkatone (24)	320±11	10
	α-Ionone (25)	205±6	25
	β-Ionone (26)	180±16	20
Heteroaromatic	Coumarine (27)	–	–
	Naphthalene (28)	–	–
	Indole (29)	25±3	<5
Steroids	Testosterone (30)	–	–

– No spin-state shift observed. (+) A spin-state shift was observed for these substances, but a binding constant could not be calculated, since substance solubility reached its limit before complete saturation of CYP109B1 was achieved

[a] Estimated to within ≤5%

verted by CYP109B1 as reported previously (Agematu et al. 2006; Girhard et al. 2009). Furthermore, when the product of the (+)-valencene **23** conversion—(+)-nootkatone **24**—was added, classical type I binding could be observed, and a K_D of 320 μM was calculated (Table 1). This phenomenon has also been reported for CYP102A1 from *B. megaterium*, which is also capable of converting (+)-valencene **23** (Sowden et al. 2005).

Reconstitution of CYP109B1 activity in vitro

CYP109B1 requires—like most P450s in general—electron transfer partners for activity. Since natural partners for CYP109B1 have not been identified yet, in vitro activity of CYP109B1 was reconstituted with various reductases and ferredoxins or flavodoxins that have been described to support activity of other P450s previously (Fig. 3). It has been shown that FdR–Fdx from *E. coli* supports the activity of P450c17 (Jenkins and Waterman 1998); bovine AdR in combination with the corresponding truncated Adx_{4-108} was used for reconstituting the steroid hydroxylase activity of bacterial CYP106A2 (Virus and Bernhardt 2008; Virus et al. 2006), and the separately expressed reductase domain of CYP102A1 (BMR) was shown to support fatty acid hydroxylating activity of CYP152A2 (Girhard et al. 2007). Furthermore, the flavodoxins YkuN and YkuP from *B. subtilis* have been reported to support activity of P450 BioI in reconstituted systems with FdR from *E. coli* (Lawson et al. 2004b). Thus, FdR–YkuN and FdR–YkuP were also tested for their ability to support activity of CYP109B1. The NAD(P)H consumption rates, coupling efficiencies, and conversions of myristic acid **5** were determined with these systems and compared to the PdR–Pdx system used previously for activity reconstitution of CYP109B1 (Table 2).

For the PdR–Pdx system, 16% conversion of myristic acid **5** was observed within 2 h at 30°C using a ratio of PdR:Pdx:CYP109B1 of 1:10:1. In comparison, conversion of myristic acid **5** was 52% with FdR–Fdx and 99% with AdR–Adx under the same conditions. For FdR–YkuN, 90% of myristic acid **5** were converted, whereas for FdR–YkuP, only 14% conversion was achieved, respectively. Systems containing BMR or FdR alone—without YkuN or YkuP—did not show any activity against myristic acid **5** (Table 2).

The overall efficiency of a reconstituted system depends *inter alia* on its NAD(P)H consumption rate and its coupling efficiency. Since two independent proteins were used for electron supply to CYP109B1, a loss of electrons can occur either between the reductase and the ferre-/flavodoxin and/or between the ferre-/flavodoxin and CYP109B1. In both cases, it results in uncoupling between NAD(P)H consumption and product formation. Similar NADPH consumption rates of ~20 nmol (nmol CYP)$^{-1}$ min^{-1} were seen for AdR–Adx, FdR–YkuP, and FdR–YkuN; the coupling efficiencies of these systems, however, differed strongly from each other (Table 2). The highest coupling of 45.8% was observed for AdR–Adx, whereas coupling for FdR–YkuP was 12.3% and for FdR–YkuP 1.8% only. If one compares the conversion values achieved for myristic acid **5** under regeneration of NAD(P)H, where the cofactor was not rate limiting, it is obvious that the

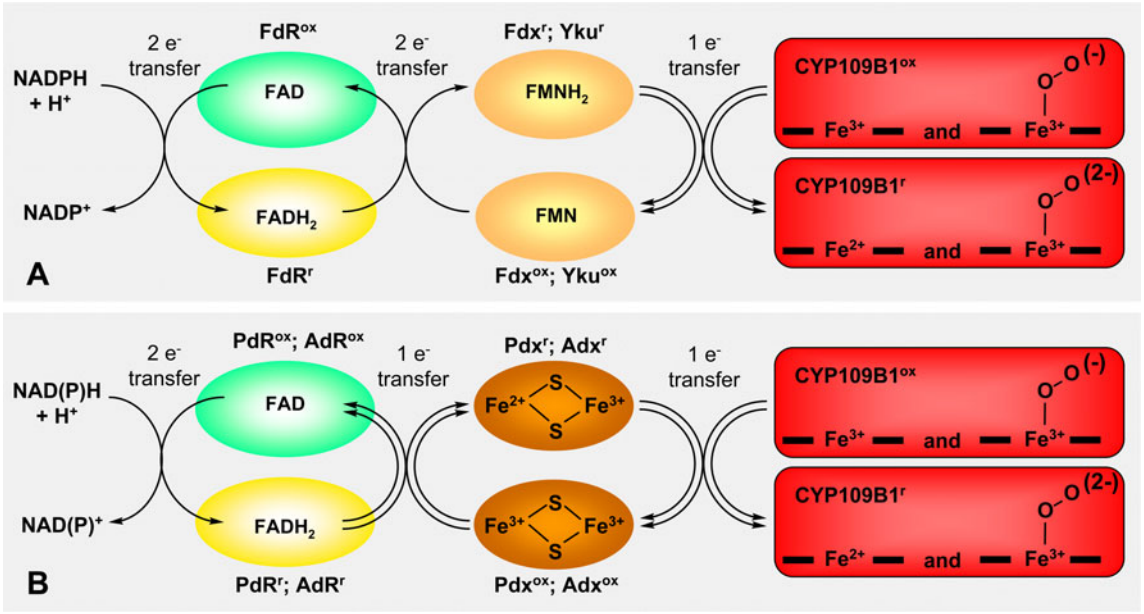

Fig. 3 Schematic organization of different redox systems for CYP109B1 applied in this study and their classification according to Hannemann et al. (2007). **a** FdR–Fdx, FdR–YkuN, and FdR–YkuP (class III, bacterial systems); **b** PdR–Pdx (class I, bacterial system) and AdR–$Adx_{4–108}$ (class I, mitochondrial system). The BMR system was not included since it did not support activity of CYP109B1. ^{ox}, oxidized form of the respective enzyme; ^{r}, reduced form

coupling efficiency of a reconstituted system is of greater importance for overall performance than the corresponding NAD(P)H consumption rate.

We also determined the conversion of (+)-valencene **23** with the reconstituted systems. In general, lower conversions than of myristic acid **5** were reached, but the tendency was similar. For (+)-valencene **23**, 10% conversion was observed with PdR–Pdx and in comparison, 17% and 23% with FdR–Fdx and AdR–Adx, respectively. For FdR–YkuN and FdR–YkuP, conversions were 26% and <1% (data not shown).

Table 2 NAD(P)H consumption, coupling, and conversion of myristic acid **5** by CYP109B1 in reconstituted enzyme systems with a ratio of reductase/ferredoxin(flavodoxin)/CYP109B1 of 1:10:1

Reconstituted system	NAD(P)H consumption rate[a]	Coupling (%)	Conversion (%)[b]
PdR–Pdx	6.6±0.3	2.4±0.3	16.0±1.4
BMR	7.3±0.4	0.0	0.0
AdR–Adx	20.2±1.2	45.8±3.5	99.1±0.7
FdR–Fdx	3.0±0.1	7.5±0.9	52.3±4.0
FdR–YkuP	20.3±1.0	1.8±0.1	13.9±0.9
FdR–YkuN	19.3±0.2	12.3±0.5	90.2±6.6

[a] Rates are given in nanomoles per (nanomoles CYP109B1) per minute; the background consumption rate with CYP109B1 alone was 0.6±0.1

[b] Conversion was determined after 2 h with NAD(P)H regeneration

From the reconstituted systems tested, AdR–Adx and FdR–YkuN are more efficient electron transfer partners than PdR–Pdx, FdR–Fdx, and FdR–YkuP, as they demonstrate higher NAD(P)H consumption rates, higher coupling, and hence, significantly higher conversions were achieved.

The flavodoxin YkuN can be considered as a potential natural redox partner for CYP109B1 in *B. subtilis*; however, in the absence of the appropriate reductase from the same strain, this hypothesis cannot be proved. Nevertheless, since the relative ratios of P450 to redox partner play an important role for the overall rate of substrate oxidation, an empirical approach with FdR–YkuN was undertaken in order to improve the substrate oxidation rates while conserving enzyme. As the rate-limiting step in P450-mediated oxidation is often the transfer of the second electron to an oxy-P450-substrate complex, we aimed to maximize the concentration of reduced YkuN by varying its concentration and that of FdR. When conversion of myristic acid **5** and (+)-valencene **23** was investigated with these systems, it was observed that the YkuN concentration represented a bottleneck for the in vitro activity reconstitution of CYP109B1. For example, the conversion of (+)-valencene **23** increased from 10% up to ~30%, when the ratio was changed from 1:1:1 to 1:20:1 (Table 3). Further increase of the flavodoxin concentration up to a ratio of 1:40:1 resulted, however, in only slightly higher conversion of ~31%, which means that electron transfer by YkuN was

Table 3 Conversion of myristic acid **5** and (+)-valencene **23** by CYP109B1 in reconstituted FdR–YkuN systems with varying ratios of redox partner proteins

FdR:YkuN:CYP [μM]	Conversion (%)[a]	
	Myristic acid **5**	(+)-Valencene **23**
1:0:1	–	–
1:1:1	38.5	10.0
1:2:1	70.2	10.8
1:5:1	88.7	19.3
1:10:1	90.2	25.5
1:20:1	nd	30.1
1:40:1	nd	31.2
2:5:1	86.3	20.6
2:10:1	94.0	26.2
2:20:1	nd	29.0
2:40:1	nd	34.2
10:10:1	93.5	26.4

– No conversion; *nd* not determined

[a] Conversion was determined after 2 h with NAD(P)H regeneration; values represent the mean of three experiments, with standard deviations within ≤10% of the mean

not rate limiting any longer. It was also observed that additional FdR did not show any significant increase in the conversion of (+)-valencene **23**. A similar tendency was observed during oxidation of myristic acid **5**. However, taking into account that the conversions achieved with FdR–YkuN were still lower than those achieved with AdR–Adx and that high amounts of YkuN were needed, the AdR–Adx system was used for further experiments.

Conversion of fatty acids

The ability to oxidize fatty acids is well known for a variety of bacterial P450s. Among well-characterized fatty acid hydroxylases are the natural fusion enzymes from the CYP102A-family, namely CYP102A1 ($P450_{BM-3}$) from *B. megaterium* (Miura and Fulco 1975) and its two homologues from *B. subtilis*, CYP102A2 (Budde et al. 2004) and CYP102A3 (Gustafsson et al. 2004).

CYP109B1 was found to oxidize saturated fatty acids with a chain length ranging from C10 to C18. Highest conversions of more than 98% were achieved for tridecanoic **4** (C13), myristic **5** (C14), and pentadecanoic acid **6** (C15), whereas conversion decreased for the substrates of shorter or longer chain length (Table S4 of the Electronic Supplementary Material). Interestingly, there was no obvious correlation between the measured substrate dissociation constants and the achieved conversions. Palmitic acid **7** (C16), for example, for which the lowest K_D value was determined, was oxidized by only 51%.

The products of fatty acid oxidations were identified by their characteristic mass fragmentation patterns after derivatization with trimethylchlorosilane (Fig. S3 of the Electronic Supplementary Material). The GC/MS analysis demonstrated that CYP109B1 hydroxylates fatty acids at subterminal positions yielding mono-hydroxylated products exclusively. Quantitative analysis of these products revealed that the carbon atoms C11 and C12 counted from the carboxyl group of all fatty acids were preferred for hydroxylation independently on chain length.

Further, we checked activity of CYP109B1 toward methyl **9–11** or ethyl esters **12**, **13** of fatty acids. Surprisingly, the monooxygenase was active toward these substrates, but with lower activity (Table S4). For example, 95% of lauric acid **3** but only 78% of the corresponding methyl ester **9** and 32% of the ethyl ester **12** were converted. A similar tendency (99% versus 80% and 34%, respectively) was observed for myristic acid **5** and its esters **10**, **13**. The regioselectivities of the hydroxylation observed for the esterified fatty acids was identical to those of the respective nonesterified fatty acid.

All unsaturated fatty acids tested (**14–16**) were oxidized by CYP109B1 with high activities (>95% within 15 min). Qualitative GC/MS analysis revealed that the oxidation proceeded unselectively resulting in more than 20 products for each substrate, which mostly could not be identified (and therefore are not included).

Conversion of *n*-alkanes and primary *n*-alcohols

Hydroxylation of alkanes has been described for a variety of P450s and generated mutants thereof (Bernhardt 2006 and references cited therein). Furthermore, primary *n*-alcohols are reported as P450 substrates as well, for example, 1-dodecanol **18** is hydroxylated at seven different positions by P450s from the white-rot fungus *Phanerochaete chrysosporium* (Matsuzaki and Wariishi 2004) and 1-tetradecanol **19** is oxidized by CYP102A1 at position ω_{-1} to ω_{-3}, with preference for the ω_{-2} carbon atom (Miura and Fulco 1975). Therefore, the *n*-alkanes decane **20** (C10), dodecane **21** (C12), and tetradecane **22** (C14) and their 1-hydroxylated derivatives 1-decanol **17**, 1-dodecanol **18**, and 1-tetradecanol **19** were investigated as potential substrates for CYP109B1.

CYP109B1 did not show any activity against the tested *n*-alkanes **20–22**, but hydroxylated 1-dodecanol **18** and 1-tetradecanol **19** at six different subterminal carbon atoms (ω_{-1} to ω_{-6}), with similar regioselectivity for both substrates (Table 4). Conversion of 1-tetradecanol **19** was slightly lower as compared with 1-dodecanol **18** (12% and 17%, respectively). 1-Decanol **17** was oxidized with high activity (99.5% conversion) at subterminal ω_{-1} to ω_{-5} positions. The terminal carbon atom of any of the alcohols

Table 4 Product distribution and conversion of primary *n*-alcohols **17–19** by CYP109B1

Chain length (no.)	Conversion (%)	Regioselectivity (%)[a]					
		ω_{-6}	ω_{-5}	ω_{-4}	ω_{-3}	ω_{-2}	ω_{-1}
10 (**17**)	99.5±0.2	–	2.9	7.2	22.2	40.5	27.3
12 (**18**)	16.6±3.1	4.4	4.9	17.4	18.7	27.2	27.5
14 (**19**)	11.8±0.3	5.9	6.7	18.8	17.1	26.8	24.9

– Compound was not observed or below the detection limits (1 μmol l^{-1})

[a] Values represent percentage of the total product and are the mean of three experiments, with standard deviations within ≤5% of the mean

was not oxidized and—in contrast to fatty acids—there was always a preference for hydroxylation at the ω_{-2} carbon atom, independent from the chain length (Table 4). Furthermore, the regioselectivities of hydroxylation of 1-decanol **17** and capric acid **2** were completely different, since capric acid **2** was oxidized at ω_{-1} position exclusively.

Conversions for 1-dodecanol **18** and 1-tetradecanol **19** were much lower than those for the corresponding fatty acids, lauric **3**, and myristic acid **5** and also lower than those of the corresponding fatty acid esters **9**, **10**, **12**, **13**, whereas conversion of 1-decanol **17** was significantly higher than those of capric acid **2**.

Conversion of ionones

Ionones are valuable fragrance constituents and therefore have attracted attention of flavor and fragrance industries, like manufacturers of perfumes, cosmetics, and other fine chemicals. Their oxygenated derivatives are sought-after building blocks, for example, 4-hydroxy-β-ionone **32**, which is an important intermediate for the synthesis of carotenoids or the plant hormone abscisic acid (Meyer 2002). CYP109B1 was shown to oxidize the sesquiterpenoid analogs α-ionone **25** and β-ionone **26** with high activity. Using AdR–Adx, the conversion achieved 70% (±6%) for α-ionone **25** and 91% (±2%) for β-ionone **26**, within 2 h.

Furthermore, a single product peak was observed by GC/MS analysis on an achiral column for each of the substrates, correspondingly (Fig. 4). For β-ionone **26**, the oxidation product was identified as 4-hydroxy-β-ionone **32** by comparison of the MS with those of an authentic reference substance reported previously (Urlacher et al. 2006). For α-ionone **25**, the oxidation product was identified as 3-hydroxy-α-ionone **31** in the same way by comparison with MS reported elsewhere (Celik et al. 2005). Since conversion of racemic α-ionone **25** was higher than 50%, obviously both enantiomers were converted by CYP109B1. The unselective hydroxylation of racemic α-ionone **25** should result in a mixture of four diastereoisomers, and consequently, two isomers would be detected by achiral analysis (Celik et al. 2005). The observed single peak might indicate that the enzyme is enantioselective. However, this aspect requires further detailed investigation.

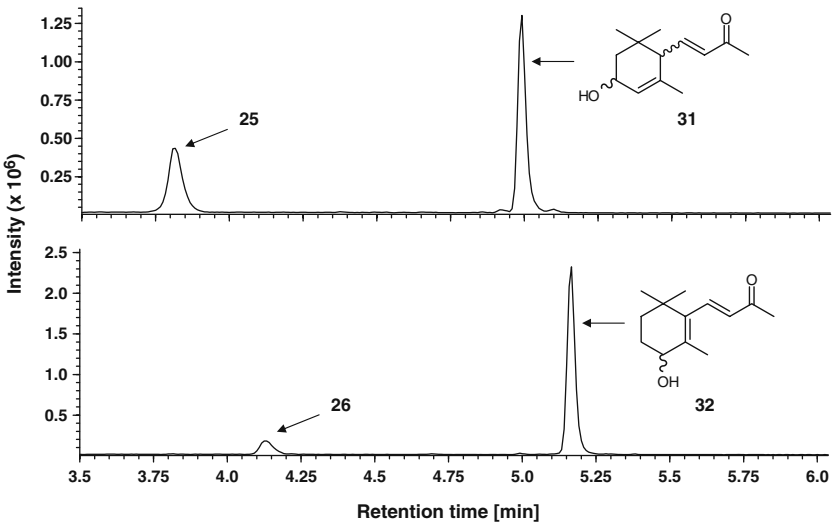

Fig. 4 GC diagram of α-ionone **25** and β-ionone **26** conversions by CYP109B1. The reaction products were identified as 3-hydroxy-α-ionone **31** and 4-hydroxy-β-ionone **32**

Indole, coumarine, and naphthalene

CYP109B1 did not show any activity toward coumarine **27** and naphthalene **28** regardless of the redox system applied. Indole induced a change of the heme spin state from low spin in the absence of substrate to only 3% high spin. Consequently, no activity toward indole **29** was observed, although this compound shows a high affinity to CYP109B1 confirmed by the low K_D value of 24.5 μM.

Since indole **29** binds to CYP109B1, but is not oxidized, we investigated if it could serve as competitive inhibitor for CYP109B1. Conversion of myristic acid **5**—whose K_D is approximately 50-fold higher than those of indole **29**—was monitored under addition of indole **29**. As expected, the presence of indole **29** in the reaction mixture drastically reduced the conversion of myristic acid **5** by CYP109B1 (Fig. 5). For example, when equal amounts (200 μM) of myristic acid **5** and indole **29** were present in the reaction mixture, the conversion dropped from ~94% (negative control without indole **29**) to ~64%. Higher amounts of indole **29** reduced conversion even further; only 20% of myristic acid **5** were converted in the presence of 10 mM indole **29**. Indole can thus be referred to as a competitive inhibitor for CYP109B1. Binding of an inhibitor to a P450 enzyme would normally result in a type II binding spectrum, with a Soret maximum at 425–435 nm and a trough at 39–405 nm (Correia and Oritz de Montellano 2005), whereas binding of indole **29** by CYP109B1 gave clearly type I binding spectra (data not shown).

Discussion

With increasing availability of genome sequences and sophisticated heterologous expression methods, new P450s identified by bioinformatics methods are readily expressed and isolated. These new enzymes will greatly expand the range of compounds that can be oxidized but equally important are the different product selectivities of existing enzymes. Therefore, for the identification of biotechnologically relevant enzymes, genome mining should be supported by substrate profiling and functional characterization of candidate P450s. Since many P450 genes are found without their associated electron transfer proteins immediately upstream or downstream, substrate spectra of such P450s cannot be identified. In some cases, the search among annotated possible candidates from the same genome yields effective electron transfer systems for P450s (Ewen et al. 2009; Mandai et al. 2009). If no potential "natural" candidates are found within the genome, however, known electron transfer proteins for other P450s can be applied because they often demonstrate "cross" interaction with foreign P450s and support their catalysis. The ability to accept electrons from "artificial" flavodoxins and ferredoxins and to display "cross" activities have been reported for several P450 monooxygenases (Bell et al. 2009; Bell and Wong 2007; Goni et al. 2009).

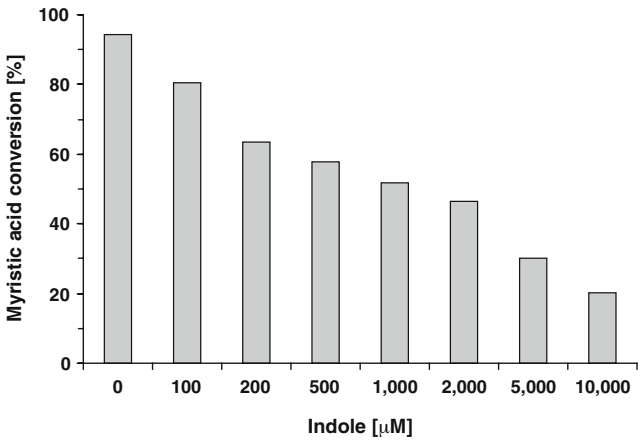

Fig. 5 Inhibition of myristic acid **5** oxidation by CYP109B1 through indole **29**. Conversion was carried out for 1 h at 30°C employing the AdR–Adx system. The data represent the average values of two experiments carried out in triplicates

Our results demonstrate that the activity of CYP109B1 can be supported by a FAD-containing reductase and either by a FMN-containing flavodoxin or a [2Fe-2S]-containing ferredoxin. The best results for CYP109B1 were observed with bovine AdR and truncated $Adx_{4–108}$, while activity with putidaredoxin and putidaredoxin reductase from *P. putida* was quite low. Both electron transfer systems belong to the class I of the P450 systems. CYP109B1 also demonstrated activity in combination with one of the two FMN-containing flavodoxins from *B. subtilis* (YkuN) but does not interact with the diflavin reductase of CYP102A1. YkuN can represent a natural electron transfer protein for CYP109B1; however, in combination with the "artificial" reductase from *E. coli*, the overall activity of the reconstituted system was lower compared to AdR–Adx. Structural and thermodynamic characterization of CYP109B1 combined with YkuN should provide insights into the flavodoxin–P450 interaction and are topic of further investigations. As possible candidate, the 4Fe-4S ferredoxin from *B. subtilis* will be also tested (Green et al. 2003).

Supported by "artificial" electron transfer partners, CYP109B1 catalyzes oxidation of a broad range of chemically different substrates. Unsaturated fatty acids were oxidized with high activity but low regioselectivity leading to a mixture of numerous products. Upon oxidation of saturated fatty acids and esterified saturated fatty acids, the carbon atoms C11 and C12 counted from the carboxyl group of all substrates were always preferred for hydroxylation, independently on chain length. Moreover, the same regioselectivity of CYP109B1 was observed during hydroxylation of esterified fatty acids. This might indicate that

the carboxyl group of fatty acids is not as crucial for substrate recognition by CYP109B1.

Interestingly, CYP109B1 hydroxylates primary *n*-alcohols of the corresponding chain length with completely different regioselectivities, preferring ω_{-2} position. A possible explanation could be that CYP109B1 possesses alternative binding sites or orientations for primary *n*-alcohols and fatty acids.

In contrast to the acyclic substrates, the cyclic sesquiterpenoid analogs α-ionone and β-ionone were hydroxylated at secondary allylic position with 100% regioselectivity, which in the case of β-ionone to our best knowledge has been described only for the mutated $P450_{BM-3}$ A74E F87V P368S (Urlacher et al. 2006). The reason for the high regioselectivity of CYP109B1 for oxidation of ionones might be caused by electronic activation of the secondary allylic carbon atoms. In the case of α-ionone, the carbon atom C3 next to the double bond between C4=C5 is most susceptible to an oxidative attack by CYP109B1, while for β-ionone this holds true for C4 next to the C5=C6 double bond. A similar preference for allylic oxidation has been described previously for the oxidation of (+)-valencene by CYP109B1, which was oxidized with high regioselectivity at allylic C2 position (Girhard et al. 2009). Thus, CYP109B1 seems to be an attractive candidate for selective oxidation of terpenes, generating valuable compounds for flavor and fragrance industries. Especially the combination of CYP109B1 with the AdR–Adx redox system could be valuable for biotechnological applications in a whole-cell bioconversion as shown before for steroid hydroxylation using CYP106A2 together with this redox system (Hannemann et al. 2006).

Acknowledgments We wish to thank Kyoko Momoi, Sumire Honda Malca, and Svetlana Tihovsky (Universitaet Stuttgart) for their help in preparation of Fdx and cloning of FdR, YkuN, and YkuP. We are also thankful to Wolfgang Reinle for expression and purification of Adx and AdR. MG, TK, and VBU acknowledge the support of this work by Deutsche Forschungsgemeinschaft (SFB706) and Ministerium für Wissenschaft, Forschung und Kunst Baden-Württemberg.

Conflict of interest The authors declare that they have no conflict of interest.

References

Agematu H, Matsumoto N, Fujii Y, Kabumoto H, Doi S, Machida K, Ishikawa J, Arisawa A (2006) Hydroxylation of testosterone by bacterial cytochromes P450 using the Escherichia coli expression system. Biosci Biotechnol Biochem 70:307–311

Arisawa A, Agematu H (2007) A modular approach to biotransformation using microbial cytochrome P450 monooxygenases. In: Schmid RD, Urlacher VB (eds) Modern biooxidation, 1st edn. Wiley-VCH, Weinheim, pp 177–192

Bell SG, Wong LL (2007) P450 enzymes from the bacterium Novosphingobium aromaticivorans. Biochem Biophys Res Commun 360:666–672

Bell SG, Dale A, Rees NH, Wong LL (2009) A cytochrome P450 class I electron transfer system from Novosphingobium aromaticivorans. Appl Microbiol Biotechnol. doi:10.1007/s00253-009-2234-y

Bernhardt R (2006) Cytochromes P450 as versatile biocatalysts. J Biotechnol 124:128–145

Budde M, Maurer SC, Schmid RD, Urlacher VB (2004) Cloning, expression and characterisation of CYP102A2, a self-sufficient P450 monooxygenase from Bacillus subtilis. Appl Microbiol Biotechnol 66:180–186

Celik A, Flitsch SL, Turner NJ (2005) Efficient terpene hydroxylation catalysts based upon P450 enzymes derived from actinomycetes. Org Biomol Chem 3:2930–2934

Chu JW, Kimura T (1973) Studies on adrenal steroid hydroxylases. Molecular and catalytic properties of adrenodoxin reductase (a flavoprotein). J Biol Chem 248:2089–2094

Correia MA, Oritz de Montellano PR (2005) Inhibition of cytochrome P450 enzymes. In: Oritz de Montellano PR (ed) Cytochrome P450: structure, mechanism, and biochemistry, 3rd edn. Springer, Berlin, pp 247–322

Cryle MJ, Stok JE, De Voss JJ (2003) Reactions catalyzed by bacterial cytochromes P450. Aust J Chem 56:749–762

Endo H, Yonetani Y, Mizoguchi H, Hashimoto S, Ozaki A (2000) Process for producing HMG-CoA reductase inhibitor. Patent WO/2000/044886

Ewen KM, Hannemann F, Khatri Y, Perlova O, Kappl R, Krug D, Huttermann J, Muller R, Bernhardt R (2009) Genome mining in Sorangium cellulosum So ce56: identification and characterization of the homologous electron transfer proteins of a myxobacterial cytochrome P450. J Biol Chem 284:28590–28598

Fischer M, Knoll M, Sirim D, Wagner F, Funke S, Pleiss J (2007) The cytochrome P450 engineering database: a navigation and prediction tool for the cytochrome P450 protein family. Bioinformatics 23:2015–2017

Fraatz MA, Berger RG, Zorn H (2009) Nootkatone—a biotechnological challenge. Appl Microbiol Biotechnol 83:35–41

Fujii K, Huennekens FM (1974) Activation of methionine synthetase by a reduced triphosphopyridine nucleotide-dependent flavoprotein system. J Biol Chem 249:6745–6753

Furuya T, Nishi T, Shibata D, Suzuki H, Ohta D, Kino K (2008) Characterization of orphan monooxygenases by rapid substrate screening using FT-ICR mass spectrometry. Chem Biol 15:563–572

Girhard M, Schuster S, Dietrich M, Durre P, Urlacher VB (2007) Cytochrome P450 monooxygenase from Clostridium acetobutylicum: a new alpha-fatty acid hydroxylase. Biochem Biophys Res Commun 362:114–119

Girhard M, Machida K, Itoh M, Schmid RD, Arisawa A, Urlacher VB (2009) Regioselective biooxidation of (+)-valencene by recombinant E. coli expressing CYP109B1 from Bacillus subtilis in a two-liquid-phase system. Microb Cell Fact 8:36

Goni G, Zollner A, Lisurek M, Velazquez-Campoy A, Pinto S, Gomez-Moreno C, Hannemann F, Bernhardt R, Medina M (2009) Cyanobacterial electron carrier proteins as electron donors to CYP106A2 from Bacillus megaterium ATCC 13368. Biochim Biophys Acta 1794:1635–1642

Green AJ, Munro AW, Cheesman MR, Reid GA, von Wachenfeldt C, Chapman SK (2003) Expression, purification and characterisation of a Bacillus subtilis ferredoxin: a potential electron transfer donor to cytochrome P450 BioI. J Inorg Biochem 93:92–99

Gustafsson MC, Roitel O, Marshall KR, Noble MA, Chapman SK, Pessegueiro A, Fulco AJ, Cheesman MR, von Wachenfeldt C, Munro AW (2004) Expression, purification, and characterization of Bacillus subtilis cytochromes P450 CYP102A2 and CYP102A3: flavocytochrome homologues of P450 BM3 from Bacillus megaterium. Biochemistry 43:5474–5487

Hannemann F, Bera AK, Fischer B, Lisurek M, Teuchner K, Bernhardt R (2002) Unfolding and conformational studies on bovine adrenodoxin probed by engineered intrinsic tryptophan fluorescence. Biochemistry 41:11008–11016

Hannemann F, Virus C, Bernhardt R (2006) Design of an Escherichia coli system for whole cell mediated steroid synthesis and molecular evolution of steroid hydroxylases. J Biotechnol 124: 172–181

Hannemann F, Bichet A, Ewen KM, Bernhardt R (2007) Cytochrome P450 systems—biological variations of electron transport chains. Biochim Biophys Acta 1770:330–344

Huang JJ, Kimura T (1973) Studies on adrenal steroid hydroxylases. Oxidation–reduction properties of adrenal iron–sulfur protein (adrenodoxin). Biochemistry 12:406–409

Jenkins CM, Waterman MR (1998) NADPH-flavodoxin reductase and flavodoxin from Escherichia coli: characteristics as a soluble microsomal P450 reductase. Biochemistry 37:6106–6113

Kunst F, Ogasawara N, Moszer I, Albertini AM, Alloni G, Azevedo V, Bertero MG, Bessieres P, Bolotin A, Borchert S, Borriss R, Boursier L, Brans A, Braun M, Brignell SC, Bron S, Brouillet S, Bruschi CV, Caldwell B, Capuano V, Carter NM, Choi SK, Codani JJ, Connerton IF, Danchin A et al (1997) The complete genome sequence of the gram-positive bacterium Bacillus subtilis. Nature 390:249–256

Lawson RJ, Leys D, Sutcliffe MJ, Kemp CA, Cheesman MR, Smith SJ, Clarkson J, Smith WE, Haq I, Perkins JB, Munro AW (2004a) Thermodynamic and biophysical characterization of cytochrome P450 BioI from Bacillus subtilis. Biochemistry 43:12410–12426

Lawson RJ, von Wachenfeldt C, Haq I, Perkins J, Munro AW (2004b) Expression and characterization of the two flavodoxin proteins of Bacillus subtilis, YkuN and YkuP: biophysical properties and interactions with cytochrome P450 BioI. Biochemistry 43:12390–12409

Mandai T, Fujiwara S, Imaoka S (2009) A novel electron transport system for thermostable CYP175A1 from Thermus thermophilus HB27. Febs J 276:2416–2429

Matsuzaki F, Wariishi H (2004) Functional diversity of cytochrome P450s of the white-rot fungus Phanerochaete chrysosporium. Biochem Biophys Res Commun 324:387–393

Maurer S, Urlacher V, Schulze H, Schmid RD (2003) Immobilisation of P450 BM-3 and an NADP+ cofactor recycling system: towards a technical application of heme-containing monooxygenases in fine chemical synthesis. Adv Synth Catal 345:802–810

McIver L, Leadbeater C, Campopiano DJ, Baxter RL, Daff SN, Chapman SK, Munro AW (1998) Characterisation of flavodoxin NADP+ oxidoreductase and flavodoxin; key components of electron transfer in Escherichia coli. Eur J Biochem 257:577–585

Meyer K (2002) Colorful antioxidants—carotenoids: significance and technical syntheses. Chem Unserer Zeit 36:178–192

Miura Y, Fulco AJ (1975) Omega-1, Omega-2 and Omega-3 hydroxylation of long-chain fatty acids, amides and alcohols by a soluble enzyme system from Bacillus megaterium. Biochim Biophys Acta 388:305–317

Nelson DR (2006) Cytochrome P450 nomenclature, 2004. Methods Mol Biol 320:1–10

Omura T, Sato R (1964a) The carbon monoxide-binding pigment of liver microsomes. I. Evidence for its hemoprotein nature. J Biol Chem 239:2370–2378

Omura T, Sato R (1964b) The carbon monoxide-binding pigment of liver microsomes. II. Solubilization, purification, and properties. J Biol Chem 239:2379–2385

Purdy MM, Koo LS, Ortiz de Montellano PR, Klinman JP (2004) Steady-state kinetic investigation of cytochrome P450cam: interaction with redox partners and reaction with molecular oxygen. Biochemistry 43:271–281

Sagara Y, Wada A, Takata Y, Waterman MR, Sekimizu K, Horiuchi T (1993) Direct expression of adrenodoxin reductase in Escherichia coli and the functional characterization. Biol Pharm Bull 16:627–630

Sambrook J, Russell D (2001) Molecular cloning: a laboratory manual. Cold Spring Harbor Laboratory Press, New York

Schenkman JB, Sligar SG, Cinti DL (1981) Substrate interaction with cytochrome P-450. Pharmacol Ther 12:43–71

Sevrioukova I, Truan G, Peterson JA (1996) The flavoprotein domain of P450BM-3: expression, purification, and properties of the flavin adenine dinucleotide- and flavin mononucleotide-binding subdomains. Biochemistry 35:7528–7535

Sirim D, Wagner F, Lisitsa A, Pleiss J (2009) The cytochrome P450 engineering database: integration of biochemical properties. BMC Biochem 10:27

Sowden RJ, Yasmin S, Rees NH, Bell SG, Wong LL (2005) Biotransformation of the sesquiterpene (+)-valencene by cytochrome P450cam and P450BM-3. Org Biomol Chem 3:57–64

Uhlmann H, Kraft R, Bernhardt R (1994) C-terminal region of adrenodoxin affects its structural integrity and determines differences in its electron transfer function to cytochrome P-450. J Biol Chem 269:22557–22564

Urlacher VB, Makhsumkhanov A, Schmid RD (2006) Biotransformation of beta-ionone by engineered cytochrome P450 BM-3. Appl Microbiol Biotechnol 70:53–59

Virus C, Bernhardt R (2008) Molecular evolution of a steroid hydroxylating cytochrome P450 using a versatile steroid detection system for screening. Lipids 43:1133–1141

Virus C, Lisurek M, Simgen B, Hannemann F, Bernhardt R (2006) Function and engineering of the 15beta-hydroxylase CYP106A2. Biochem Soc Trans 34:1215–1218

Wang ZQ, Lawson RJ, Buddha MR, Wei CC, Crane BR, Munro AW, Stuehr DJ (2007) Bacterial flavodoxins support nitric oxide production by Bacillus subtilis nitric-oxide synthase. J Biol Chem 282:2196–2202